JEM Journal of Experimental Medicine

BRIEF DEFINITIVE REPORT

Aire-expressing ILC3-like cells in the lymph node display potent APC features

Tomoyoshi Yamano[1*], Jan Dobeš[2,3*], Matouš Vobořil[2], Madlen Steinert[1], Tomáš Brabec[2], Natalia Ziętara[1], Martina Dobešová[2], Caspar Ohnmacht[4], Martti Laan[5], Part Peterson[5], Vladimir Benes[6], Radislav Sedláček[7], Rikinari Hanayama[8], Michal Kolář[9], Ludger Klein[1*], and Dominik Filipp[2*]

The autoimmune regulator (Aire) serves an essential function for T cell tolerance by promoting the "promiscuous" expression of tissue antigens in thymic epithelial cells. Aire is also detected in rare cells in peripheral lymphoid organs, but the identity of these cells is poorly understood. Here, we report that Aire protein–expressing cells in lymph nodes exhibit typical group 3 innate lymphoid cell (ILC3) characteristics such as lymphoid morphology, absence of "classical" hematopoietic lineage markers, and dependence on RORγt. Aire$^+$ cells are more frequent among lineage-negative RORγt$^+$ cells of peripheral lymph nodes as compared with mucosa-draining lymph nodes, display a unique Aire-dependent transcriptional signature, express high surface levels of MHCII and costimulatory molecules, and efficiently present an endogenously expressed model antigen to CD4$^+$ T cells. These findings define a novel type of ILC3-like cells with potent APC features, suggesting that these cells serve a function in the control of T cell responses.

Introduction

The autoimmune regulator (Aire)'s crucial function in the promotion of promiscuous gene expression in medullary thymic epithelial cells (mTECs) is well established. mTECs express thousands of tissue-restricted antigens (TRAs) and present these on MHCI and II (Kyewski and Klein, 2006; Mathis and Benoist, 2007; Peterson et al., 2008; Klein et al., 2014). Aire deficiency strongly diminishes TRA expression in mTECs, offering an explanation how Aire mutations cause the human autoimmune polyendocrine syndrome type 1 (Husebye et al., 2018) and similar autoimmune manifestations in mice (Anderson et al., 2002; Ramsey et al., 2002).

Defective tolerance in Aire$^{-/-}$ mice also includes antigens whose expression in mTECs is Aire independent (Anderson et al., 2005; Kuroda et al., 2005; Hubert et al., 2011). This suggests that Aire coordinates mTEC functions beyond promiscuous gene expression such as mTEC differentiation (Yano et al., 2008; Nishikawa et al., 2010), cytokine and chemokine production (Yano et al., 2008; Laan et al., 2009; Lei et al., 2011; Fujikado et al., 2016), or antigen handling and presentation (Anderson et al., 2005; Hubert et al., 2011). Furthermore, it remains open how two key disease manifestations in autoimmune polyendocrine syndrome type 1 patients, candidiasis and ectodermal dystrophy, can be reconciled with Aire serving its functions exclusively in mTECs.

Fate-mapping revealed Aire expression outside mTECs during embryonic development (Nishikawa et al., 2010). In adult mice, Aire mRNA can be detected in secondary lymphoid organs and also in nonimmune cell types, but there is some controversy as to how well Aire transcripts correlate with actual protein expression (Heino et al., 2000; Halonen et al., 2001; Adamson et al., 2004; Hubert et al., 2008; Schaller et al., 2008; Gardner et al., 2009; Fletcher et al., 2010; Poliani et al., 2010). Aire reporter mice have been instrumental in the identification of a unique cell subset referred to as extrathymic Aire-expressing cells (eTACs), hematopoietic APCs that morphologically resemble dendritic cells (DCs; Gardner et al., 2008, 2013). Aire-expressing DCs have recently also been described in human tonsils (Fergusson et al., 2019).

[1]Institute for Immunology, Faculty of Medicine, Ludwig-Maximilans-Universität, Munich, Germany; [2]Laboratory of Immunobiology, Institute of Molecular Genetics of the Czech Academy of Sciences, Prague, Czech Republic; [3]Department of Cell Biology, Faculty of Science, Charles University in Prague, Prague, Czech Republic; [4]Helmholtz Zentrum München, Institut für Allergieforschung, Neuherberg, Germany; [5]Institute of Biomedicine and Translational Medicine, University of Tartu, Tartu, Estonia; [6]Genomics Core Facility, European Molecular Biology Laboratory, Services and Technology Unit, Heidelberg, Germany; [7]Czech Centre for Phenogenomics and Laboratory of Transgenic Models of Diseases, Institute of Molecular Genetics of the Czech Academy of Sciences, Prague, Czech Republic; [8]Department of Immunology, Kanazawa University Graduate School of Medical Sciences, and World Premier International Research Center Initiative Nano Life Science Institute, Kanazawa University, Ishikawa, Japan; [9]Laboratory of Genomics and Bioinformatics, Institute of Molecular Genetics of the Czech Academy of Sciences, Prague, Czech Republic.

*T. Yamano, J. Dobeš, L. Klein, and D. Filipp contributed equally to this paper; Correspondence to Ludger Klein: ludger.klein@med.lmu.de; Dominik Filipp: dominik.filipp@img.cas.cz; T. Yamano's present address is Department of Immunology, Kanazawa University Graduate School of Medical Sciences, and World Premier International Research Center Initiative Nano Life Science Institute, Kanazawa University, Ishikawa, Japan.

Here, we aimed to clarify the identity of Aire-expressing cells in lymph nodes. We identified three phenotypically distinct subsets of hematopoietic cells that expressed endogenous Aire mRNA, including the previously described EpCAM$^+$CD11c$^+$ eTACs. However, Aire protein was exclusively found in an EpCAM$^-$CD11c$^-$ innate lymphoid cell (ILC) 3–like cell type with potent APC features.

Results and discussion

We confirmed in two independent mouse strains that Aire-reporter expression in LNs was confined to MHCII$^+$ cells (Gardner et al., 2013). Surprisingly, Aire-reporter$^+$ cells not only contained cells with the reported EpCAM$^+$CD11c$^+$ "eTAC" phenotype, but also similar proportions of EpCAM$^-$CD11c$^+$ and EpCAM$^-$CD11c$^-$ cells (Figs. 1 A and S1 A). Endogenous Aire mRNA was highest in EpCAM$^-$CD11c$^-$ cells (Figs. 1 B and S1 B). Aire-protein was detectable by intracellular staining (ICS) in 10–20% of Aire-reporter$^+$EpCAM$^-$CD11c$^-$ cells, but not in the other two subsets (Figs. 1 C and S1 C). Aire was localized in nuclear dots, akin to its subcellular distribution in mTECs (Fig. 1 D).

Independent of reporter systems, Aire$^+$ LN cells were detectable by ICS, and these cells were uniformly CD45$^+$EpCAM$^-$CD11c$^-$ (Fig. 1 E). Aire-ICS$^+$ cells were found at similar frequencies in various peripheral (p)LNs, yet were less frequent in mesenteric LNs (Fig. S1 D). Their abundance was very low in newborns and reached a transient maximum in 2-wk-old mice (Fig. 1 F). Bone marrow (BM) chimeras confirmed their hematopoietic origin (Fig. 1 G).

Aire$^+$ LN cells did not express common lineage-specific surface molecules (Fig. 2 A) and contained negligible mRNA levels of signature genes specific for T or B cells, DCs, macrophages, or granulocytes (Fig. 2 B). However, they expressed genes characteristic for ILCs such as *Id2*, *Kit*, *Il7r*, *Itga4*, and *Itgb7* (Fig. 2 C; Robinette et al., 2015; Seehus et al., 2015). Of the transcription factors (TFs) that regulate the development and function of distinct ILC subsets (Spits et al., 2013), Aire$^+$EpCAM$^-$CD11c$^-$ LN cells expressed the group 3 ILC signature TF RORγt, but not or only weakly T-bet, Eomesodermin, GATA3, and RORα (Fig. 2, C and D).

Aire$^+$EpCAM$^-$CD11c$^-$ LN cells also displayed other ILC hallmarks. First, they had a typical lymphoid morphology, albeit being slightly larger than "bulk" Lin$^-$Rorγt$^+$ ILC3s from LNs, whereas Aire-reporter$^+$EpCAM$^+$CD11c$^+$ "eTACs," as previously described, resembled DCs (Fig. 2 E). Second, they were independent of *Rag* genes (Figs. 2 F and S2 A). Third, and most significantly, *Rorc*$^{-/-}$ precursors failed to give rise to Aire$^+$ LN cells in mixed [*Rorc*$^{-/-}$: *Rorc*$^{+/+}$] → *WT* BM-chimeras, indicating that these cells, like ILC3s (Eberl et al., 2004; Luci et al., 2009; Satoh-Takayama et al., 2009), intrinsically depended on RORγt for their development (Fig. 2 G). Given these commonalities between Aire$^+$ LN cells and ILC3s, we asked whether a "classical" cytometric ILC3 gating strategy including "larger" cells would comprise Aire$^+$ cells. Indeed, around 15% of Lin$^-$CD45$^+$RORγt$^+$ pLN cells were Aire-ICS$^+$ (Figs. 2 H and S2 B).

Group 3 ILCs can be subclassified based on anatomical distribution, ontogeny, and surface phenotype (Spits et al., 2013; Montaldo et al., 2015). CCR6$^+$NKp46$^-$ lymphoid tissue-inducer (LTi) cells arise embryonically and predominantly reside in secondary lymphoid tissues. Postnatally emerging ILC3s can be subdivided into CCR6$^+$NKp46$^-$ LTi-like cells and CCR6$^-$ ILC3s. LTi-like cells are the predominant population in LNs, whereas CCR6$^-$ ILC3s are most abundant in mucosal tissues. To assess how Lin$^-$RORγt$^+$Aire$^+$ cells fit into these categories, we compared their phenotype and ontogeny to Lin$^-$RORγt$^+$Aire$^-$ canonical ILC3s from pLNs. RORγt levels were similar in both cell types (Fig. S2 C). Aire$^+$ cells were also strikingly similar to canonical pLN ILC3s with regard to expression of the TF Id2, surface expression of c-Kit and CCR6, and absence of NKp46 (Fig. 2 J). However, despite sharing the CCR6$^+$NKp46$^-$ phenotype of canonical LN-ILC3s, Aire$^+$ cells were homogeneously negative for IL7Rα, CD90, and CD4, whereas expression of these molecules was heterogeneous on CCR6$^+$NKp46$^-$Aire$^-$ ILC3s (Fig. 2 J). Aire$^+$ LN cells were very rare at birth, peaked at the time of weaning, and slightly declined thereafter, whereas canonical ILC3s were abundant in neonates and decreased with age (Jones et al., 2018; Figs. 1 F and 2 K). Thus, Aire$^+$ LN cells resembled LTi-like ILC3s, yet displayed distinctive features, and from here on will be referred to as Aire$^+$ ILC3-like cells.

Aire, besides its role in TRA expression, has been suggested to control the development and/or survival of mTECs (Gray et al., 2007; Hikosaka et al., 2008; Wang et al., 2012). To address whether a lack of Aire in cells that otherwise express it would perturb their differentiation, we generated mixed [*Aire*$^{-/-}$ Aire-reporter: *Aire*$^{+/+}$ Aire-reporter] → *WT* BM-chimeras. Aire-reporter$^+$ cells that had emerged from either *Aire*$^{-/-}$ or *Aire*$^{+/+}$ precursors were present at equal frequencies. Thus, Aire is unlikely to be a developmental or homeostatic regulator of Aire$^+$ ILC3-like cells (Fig. 3 A).

Aire expression in mTECs is orchestrated by NF-κB signals that emanate from receptors of the TNF superfamily (Akiyama et al., 2012) and converge on an essential enhancer-element (CNS1) in the *Aire* gene (Haljasorg et al., 2015; LaFlam et al., 2015). Aire$^+$ LN cells were absent in *Aire-CNS1*$^{-/-}$ mice, indicating that the gene-proximal requirements for Aire expression in Aire$^+$ ILC3-like cells resemble those in mTECs (Fig. 3 B). MHCII-dependent cognate interactions of mTECs and thymic B cells with developing CD4 T cells provide a crucial platform for Aire-inducing Rank or CD40 signals (Rossi et al., 2007; Akiyama et al., 2008; Hikosaka et al., 2008; Irla et al., 2008; Roberts et al., 2012; Yamano et al., 2015). We asked whether a similar scenario applies to Aire$^+$ LN cells. In mixed [*MHCII*$^{-/-}$: *MHCII*$^{+/+}$] → *WT* BM-chimeras, MHCII-deficient precursor cells efficiently gave rise to Aire$^+$ LN cells (Fig. 3 C). Moreover, Aire$^+$ LN cells were similarly abundant in *Rag2*$^{-/-}$ mice and *WT* controls (Fig. 3 D). Thus, in contrast to what has been established for mTECs and thymic B cells, Aire$^+$ LN cells are independent of cross-talk with T cells, indicating that an "innate program" governs their cellular identity.

Given the critical role of Aire's NF-κB response element in Aire$^+$ LN cells, it was likely that extrinsic TNF receptor family signals of "nonadaptive" origin were crucial for their differentiation. Aire$^+$ LN cells emerged with equal efficacy from either *CD40*$^{-/-}$ or *CD40*$^{+/+}$ precursors (Fig. 3 E). By contrast, Rank

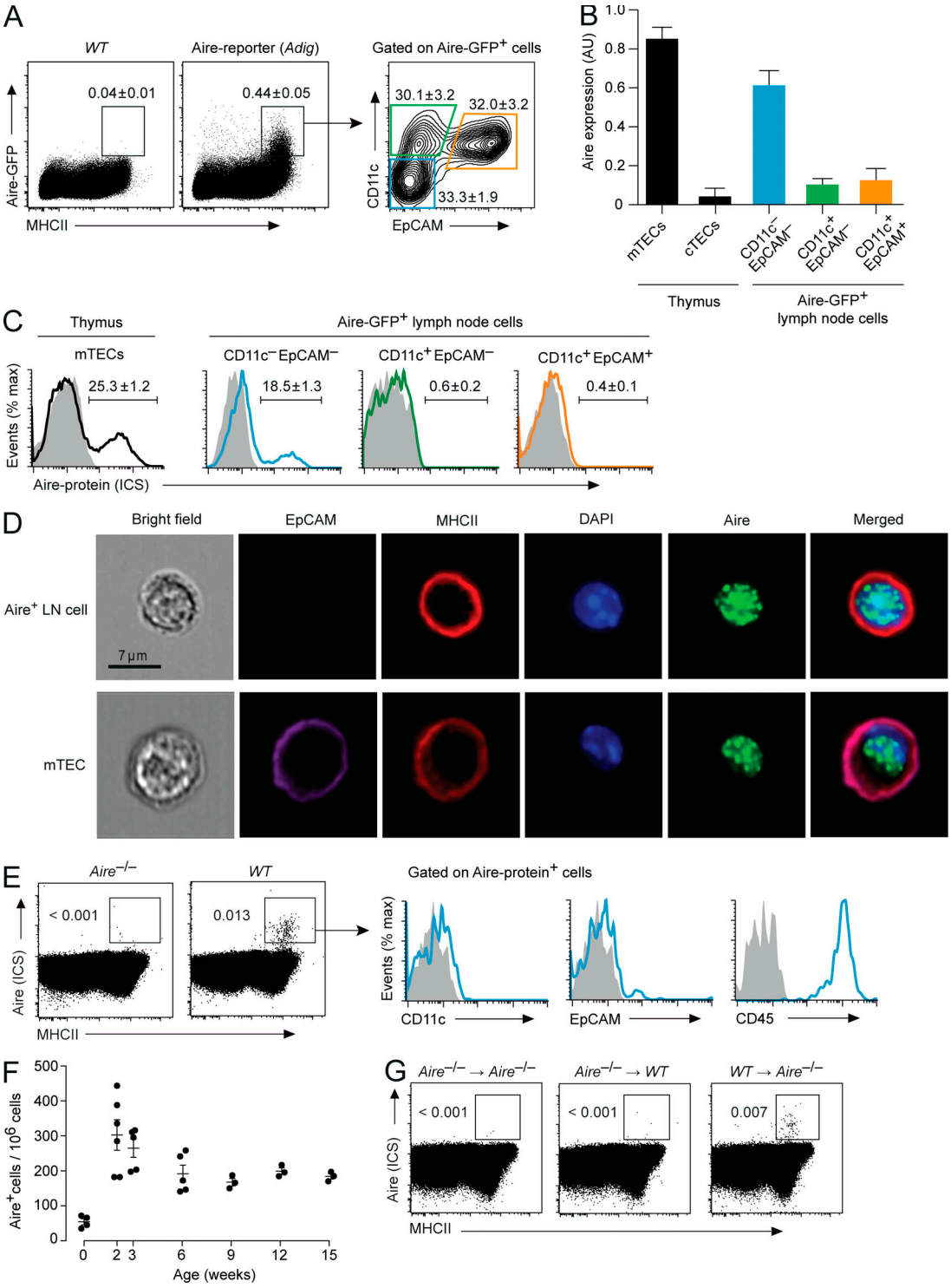

Figure 1. **Phenotype of Aire-expressing cells in LNs. (A)** Expression of GFP and MHCII in LN cells from *Adig* Aire-reporter mice and *WT* controls and staining for CD11c and EpCAM on gated Aire-GFP$^+$MHCII$^+$ cells (representative of $n \geq 4$ each). **(B)** Aire mRNA in medullary and cortical thymic epithelial cells (mTECs and cTECs, respectively) and in Aire-GFP$^+$ LN cells sorted according to expression of CD11c and EpCAM. Data are mean values ± SEM of triplicates. AU, arbitrary units. **(C)** ICS for Aire protein in subsets of Aire-GFP$^+$ LN cells. The average frequency ± SEM of Aire-ICS$^+$ cells is indicated ($n = 4$). **(D)** Nuclear localization of Aire protein and surface marker expression in Aire-expressing LN cells or mTECs visualized by imaging flow cytometry. **(E)** ICS for Aire protein and surface expression of MHCII in total LN cells from *WT* and *Aire*$^{-/-}$ mice. Histograms on the right show CD11c, EpCAM, and CD45 on gated Aire$^+$MHCII$^+$ cells (representative of $n \geq 5$). **(F)** Number of Aire$^+$ LN cells per 10^6 total pLN cells in mice of the indicated age ($n \geq 3$ each; 0 wk = 4 d old). **(G)** Aire and MHCII expression in total LN cells from *Aire*$^{-/-}$ → *Aire*$^{-/-}$, *Aire*$^{-/-}$ → *WT* or *WT* → *Aire*$^{-/-}$ BM chimeras (representative of $n \geq 4$ each).

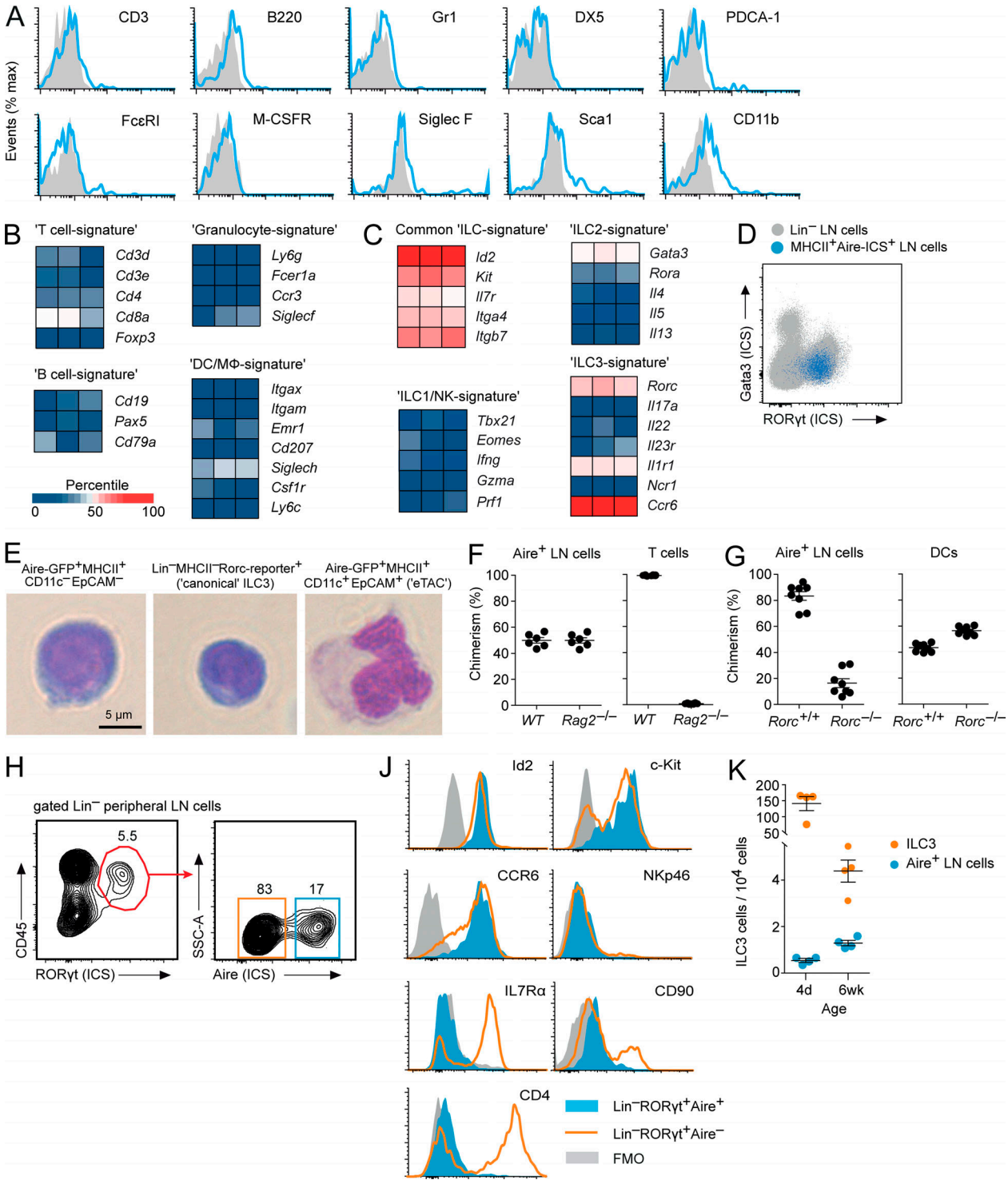

Figure 2. **Aire⁺ LN cells display ILC3 characteristics. (A)** Expression of hematopoietic lineage markers on Aire-GFP⁺MHCII⁺CD11c⁻EpCAM⁻ LN cells from *Adig* mice (representative of $n \geq 4$). **(B)** RNA expression of hematopoietic lineage-specific signature genes in Aire⁺ LN cells. **(C)** RNA expression of ILC signature genes in enriched Aire⁺ LN cells. **(D)** ICS for RORγt and Gata3 in MHCII⁺Aire⁺ LN cells (blue dots) back-gated on total Lin⁻ (CD3, CD19, B220, Gr-1, CD11c, and CD11b) LN cells (gray dots; representative of $n = 3$). **(E)** Morphology of representative Aire-GFP⁺MHCII⁺CD11c⁻EpCAM⁻ LN cells, "canonical" LN ILC3s (Lin⁻MHCII⁻RORγt⁺IL7Rα⁺), and eTACs (Aire-GFP⁺MHCII⁺EpCAM⁺ CD11c⁺). **(F)** Contribution of *WT* and *Rag2*$^{-/-}$ precursor cells to Aire-ICS⁺ LN cells or T cells in 1:1 mixed [*Rag2*$^{-/-}$: *WT*] → *WT* BM-chimeras ($n = 6$). **(G)** Contribution of *Rorc*$^{+/+}$ and *Rorc*$^{-/-}$ precursor cells to Aire-ICS⁺ cells in LN or spleen or to DCs in 1:1 mixed [*Rorc*$^{+/+}$: *Rorc*$^{-/-}$] → *WT* BM-chimeras ($n = 7$). **(H)** Gating strategy for Lin⁻ (Lin1: CD3, CD19, B220, Gr-1; Lin 2: CD11c and CD11b) RORγt⁺ LN ILC3s and expression of Aire by ICS. **(J)** Intracellular staining for Id2 protein and surface expression of c-kit, CCR6, NKp46, IL7Rα, CD90, and CD4 in Aire⁺ (filled blue histogram) and Aire⁻ (open orange histogram) Lin⁻RORγt⁺ cells (representative of $n = 3$). FMO, fluorescence minus one. **(K)** Number of "canonical" LN ILC3s (orange) and Aire⁺ LN cells (blue) in 4-d- and 6-wk-old animals ($n = 4$). Data are mean ± SEM.

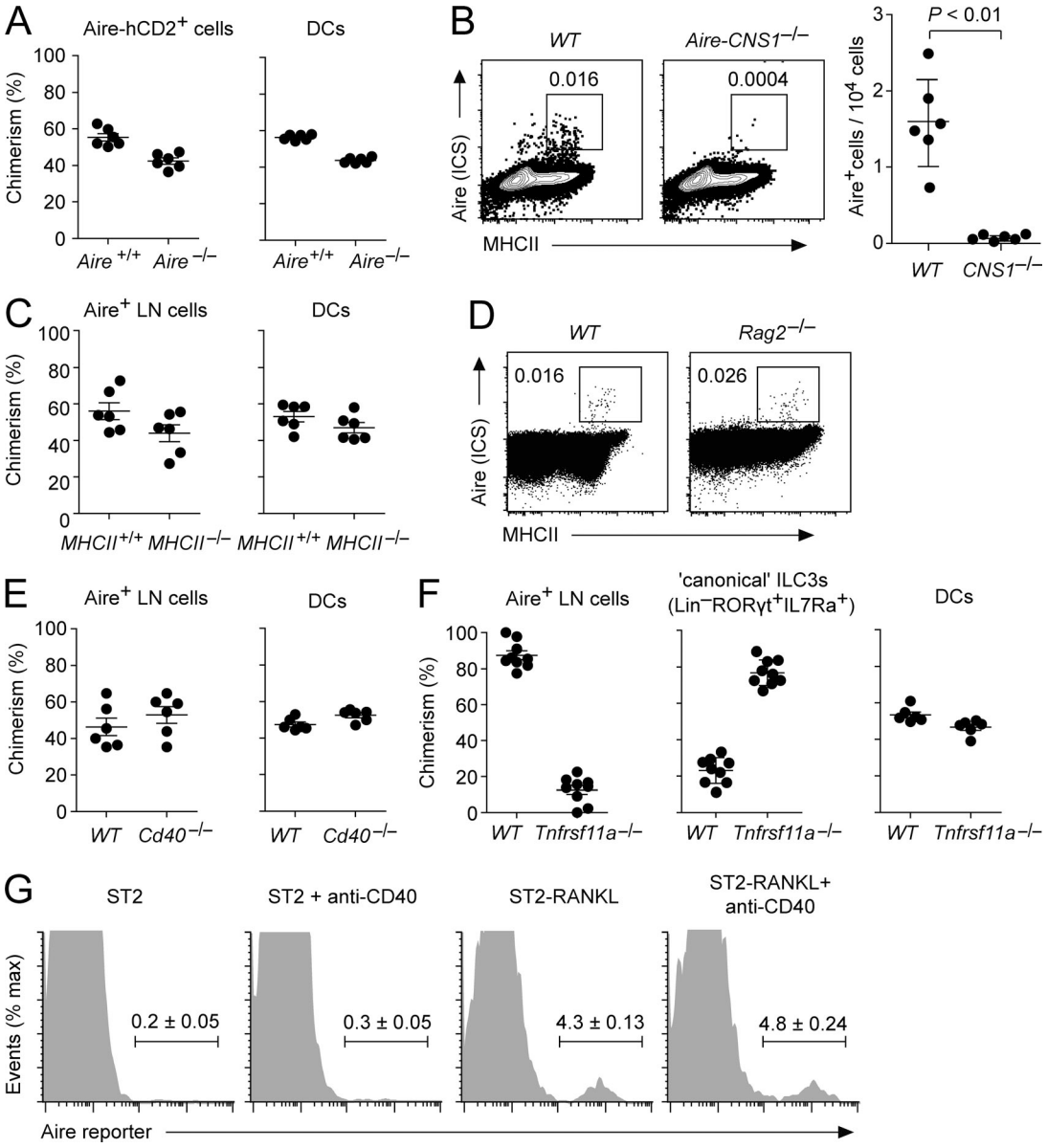

Figure 3. **Molecular and cellular requirements for Aire expression in Aire⁺ ILC3-like cells. (A)** Contribution of *Aire*$^{+/+}$ and *Aire*$^{-/-}$ precursor cells to Aire-reporter⁺ LN cells or DCs in 1:1 mixed [*Aire*$^{+/+}$ *Aire-HCO*: *Aire*$^{-/-}$ *Aire*$^{+/+}$ *Aire-HCO*] → *WT* BM-chimeras (n = 6). **(B)** Aire (ICS) and MHCII in LN cells from *WT* controls and *Aire-CNS1*$^{-/-}$ mice and number of Aire-ICS⁺MHCII⁺ cells per 10^4 LN cells (n = 6 each). **(C)** Contribution of *MHCII*$^{+/+}$ and *MHCII*$^{-/-}$ precursor cells to Aire⁺ LN cells or DCs in 1:1 mixed [*MHCII*$^{+/+}$: *MHCII*$^{-/-}$] → *WT* BM-chimeras (n = 6). **(D)** Aire (ICS) and MHCII in LN cells from *Rag2*$^{-/-}$ mice and *WT* controls ($n \geq 3$ each). **(E)** Contribution of *Cd40*$^{+/+}$ and *Cd40*$^{-/-}$ precursor cells to Aire⁺ LN cells or DCs in 1:1 mixed [*Cd40*$^{+/+}$: *Cd40*$^{-/-}$] → *WT* BM-chimeras (n = 6). **(F)** Contribution of *Tnfrsf11a*$^{+/+}$ and *Tnfrsf11a*$^{-/-}$ precursor cells to Aire⁺ LN cells, "canonical" ILC3s (Lin⁻RORγt⁺IL7Rα⁺), or DCs in 1:1 mixed [*Tnfrsf11a*$^{+/+}$: *Tnfrsf11a*$^{-/-}$] → *WT* fetal liver chimeras (n = 9). **(G)** Aire-reporter expression in "canonical" IL7Rα⁺ LN ILC3s after in vitro culture with or without agonistic anti–CD40 antibody or with ST2-RankL cells (representative of n = 3 each). Data are mean ± SEM. Student's t test was used to calculate P values.

deficiency resulted in a severe cell-intrinsic defect of hematopoietic precursors to contribute to Aire⁺ LN cells in mixed chimeras (Fig. 3 F). Intriguingly, concomitant to being virtually absent from Aire⁺ ILC3-like cells, Rank-deficient cells were strongly over-represented among canonical IL7Rα⁺ ILC3s. A possible explanation for this was that LN ILC3s under steady-state conditions differentiate into Aire⁺ ILC3-like cells upon Rank stimulation, yet accumulate when their capacity to signal via Rank is genetically ablated. In support of such a precursor/progeny relationship, in vitro culture of canonical LN ILC3s with Rank-ligand–expressing stromal cells induced Aire expression in a fraction of cells (Fig. 3 G).

RNA sequencing (RNA-seq) of Aire-reporter⁺ LN cells from WT and Aire-deficient mice revealed 707 differentially expressed transcripts (Fig. 4 A). Of these, 334 were Aire-induced, and 373 were repressed (Tables S1 and S2). Quantitative PCR analysis of selected Aire-induced or Aire-repressed genes confirmed their Aire-regulated expression (Fig. 4 B). Among Aire-induced transcripts, only 60 were classified as TRAs (Sansom et al., 2014; Fig. 4 A). Thus, in contrast to what is known for

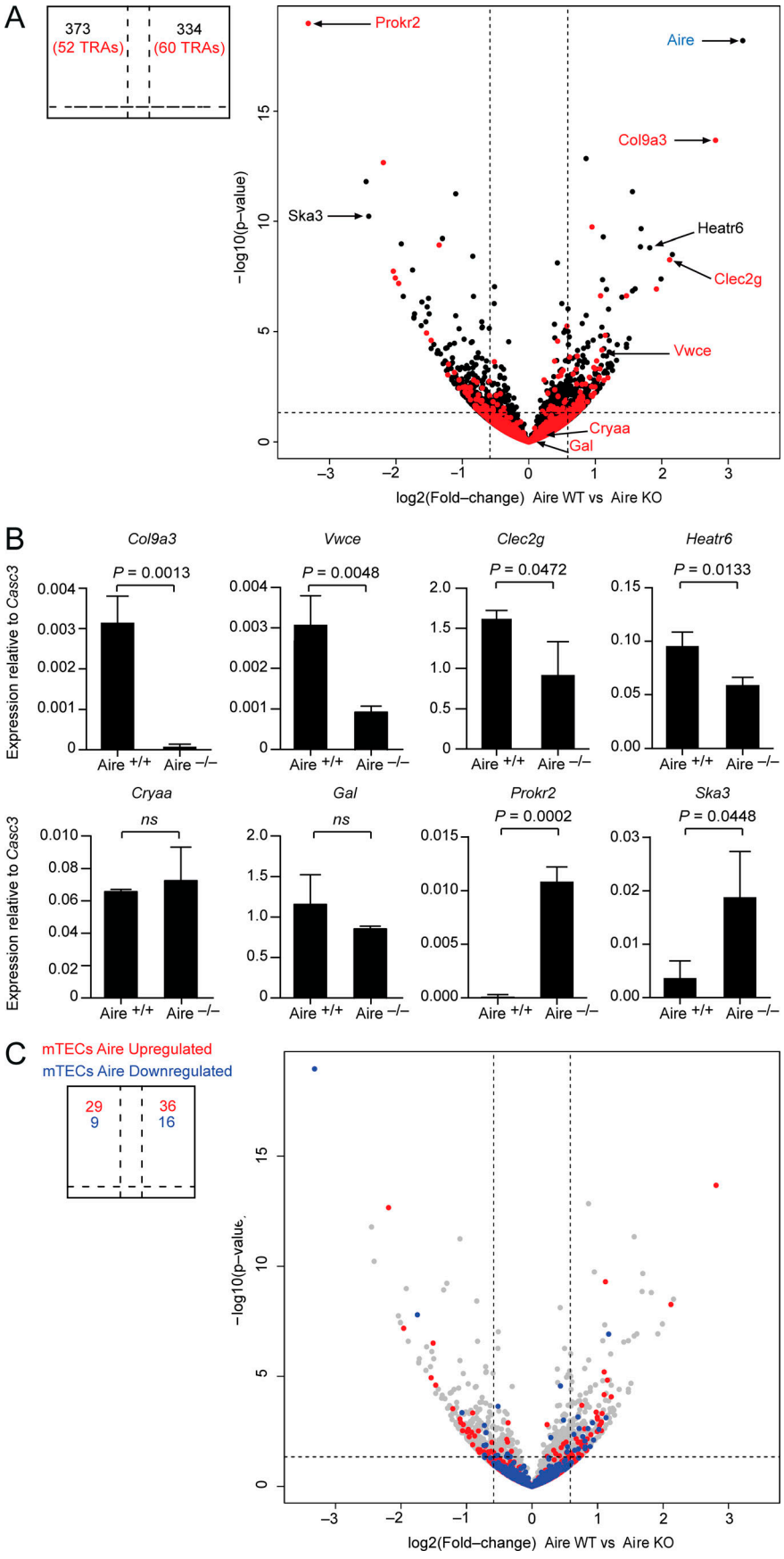

Figure 4. **Aire orchestrates a distinct genetic program in Aire⁺ ILC3-like cells. (A)** RNA-seq data from Lin⁻MHCII^{hi}CD80⁺ cells from *Aire*$^{+/+}$ and *Aire*$^{-/-}$ mice. Genes encoding for TRAs are colored in red. Fold-change cutoff: 1.5; P value: 0.05 (indicated by a dashed line). **(B)** Quantitative PCR analysis of mRNA expression of selected differentially expressed genes. Data are mean ± SD of three independent experiments. ns, not significant. **(C)** Comparison of Aire-dependent gene expression in Aire⁺ LN cells and mTECs. Genes that are up-regulated (depicted in red; 1,732 genes) or down-regulated (depicted in blue; 423 genes) by Aire in mTECs by at least 1.5-fold were projected onto the volcano plot shown in A. Student's *t* test was used to calculate P values.

mTECs (Anderson et al., 2002; Kyewski and Klein, 2006), the Aire-induced transcriptome of Aire$^+$ LN cells is not biased toward TRAs. Interestingly, Aire-regulated genes in Aire$^+$ LN cells and mTECs were largely nonoverlapping, that is, only 90 of 707 Aire-regulated transcripts in Aire$^+$ LN cells were also affected by Aire deficiency in mTECs. Moreover, many of these genes displayed opposing effects in mTECs or Aire$^+$ LN cells (Fig. 4 C). Thus, Aire controls a distinct transcriptional program in Aire$^+$ ILC3-like cells.

Aire$^+$ LN cells had high surface levels of MHCII and strongly expressed mRNAs encoding for costimulatory or coinhibitory molecules (Fig. 5 A). To relate this to canonical LN ILC3s, we directly compared the surface phenotype of Aire$^+$IL7Rα$^-$ or Aire$^-$IL7Rα$^+$ Lin$^-$CD45$^+$RORγt$^+$ LN cells (Figs. 5 B and S3 A). Aire$^+$ ILC3-like pLN cells had homogeneously high surface levels of MHCII, CD80, CD86, CD40, and Icos-L and detectable amounts of PD-L1. By contrast, with the exception of CD86, these molecules were substantially lower or absent on Aire$^-$IL7Rα$^+$ ILC3s (Fig. 5 C). We confirmed and extended these data through gating on MHCII^{hi}IL7Rα$^-$ or MHCII$^{lo/int}$IL7Rα$^+$ cells among Lin$^-$CD45$^+$RORγt$^+$ cells, which clearly separated Aire$^+$ ILC3-like cells and Aire$^-$ canonical ILC3s (Fig. S3, A and B). Consistent with our previous observations, MHCII^{hi}IL7Rα$^-$ Aire$^+$ ILC3-like cells were far more abundant in pLNs as compared with mesenteric LNs (Fig. S3, A–C), were slightly lower for CD45 (Fig. S3 D), and had much higher surface levels of APC-associated molecules as compared with MHCII$^{lo/int}$IL7Rα$^+$ cells (Fig. S3 E). Moreover, MHCII^{hi}IL7Rα$^-$ Aire$^+$ ILC3-like cells were negative for CD4, CD90, and CD25, whereas canonical ILC3s were heterogeneous for CD4 and CD90 and homogeneously positive for CD25 (Fig. S3 F).

Given the potent APC features of Aire$^+$ ILC3-like cells, we asked whether a model antigen expressed by these cells was visible to CD4 T cells. Influenza hemagglutinin (HA)–specific CD4 T cells and polyclonal "reference" T cells were adoptively transferred into *Aire-HCO* mice, which express HA from a bacterial artificial chromosome–transgenic *Aire* gene (Hinterberger et al., 2010). 14 d after transfer, HA-specific CD4 T cells were strongly diminished in *Aire-HCO* recipients but not in *WT* controls (Fig. 5 D), indicating that peripheral antigen encounter resulted in the deletion of these cells. Similar results were obtained when *Aire-HCO* → *WT* BM-chimeras were used as recipients, indicating that deletion of TCR-HA cells resulted from HA expression in the hematopoietic compartment (Fig. 5 E). To directly assess presentation of endogenously expressed HA, Aire$^+$ ILC3-like cells from *Aire-HCO* mice were cultured with HA-specific CD4 T cell hybridoma cells carrying a GFP IL-2 reporter (Aschenbrenner et al., 2007). For comparison, we performed these assays also with mTECs and EpCAM$^+$CD11c$^+$ eTACs. Aire$^+$ ILC3-like cells presented HA with similar efficacy as mTECs. By contrast, no direct presentation of HA was measurable with eTACs, despite similar expression of the Aire-reporter (Figs. 5 F and S1 A). When loaded with exogenous HA-peptide, all three cell types elicited similar responses, excluding that differential expression of MHCII accounted for these differences (Fig. 5 F).

In sum, our data suggest that Aire protein–expressing cells in mouse pLNs may represent a hitherto unknown ILC3 subset. In distinction from the majority of Lin$^-$RORγt$^+$ LN ILC3s, they do not express the IL7Rα, which, besides the absence of Aire$^+$ ILC3s from the intestine and their low frequency in mesenteric LNs, may explain why Aire expression has not been noticed in transcriptomic analyses of ILC subsets (Robinette et al., 2015; Gury-BenAri et al., 2016). It will be interesting to clarify the potential precursor progeny relationship between canonical ILC3s and Aire$^+$ LN cells and how the Rank pathway is involved. It was recently shown that Rank signaling negatively regulates the abundance and effector functions of intestinal ILC3s (Bando et al., 2018). Together with our findings, this suggests that both in pLNs as well as in the intestine, ILC3s receive tonic Rank stimulation, yet may differ with regards to the ensuing biological response.

Aire$^+$ ILC3-like cells display potent APC features, consistent with accruing evidence that ILC3s can orchestrate CD4 T cell responses. Selective ablation of MHCII molecules on RORγt$^+$ cells resulted in impaired tolerance to commensals and intestinal inflammation (Hepworth et al., 2013, 2015). Other reports linked MHCII deficiency in RORγt$^+$ cells to impaired T and B cell responses to "foreign" antigens (von Burg et al., 2014). How this relates to Aire$^+$ ILC3-like cells and under which circumstances antigen recognition on these cells may result in tolerance versus immunity remains to be seen. Along these lines, it will be interesting to see whether Aire expression in Aire$^+$ ILC3-like cells is of true physiological significance, as these cells do not recapitulate bona fide "promiscuous" TRA expression as it is seen in mTECs. It remains possible that Aire influences features of Aire$^+$ LN cells that are unrelated to TRA expression.

Materials and methods

Mice

Adig (Gardner et al., 2008), Aire-HCO (Hinterberger et al., 2010), Aire$^{-/-}$ (Ramsey et al., 2002), Aire-CNS1$^{-/-}$ (Haljasorg et al., 2015), TCR-HA (Kirberg et al., 1994), Cd40$^{-/-}$ (Kawabe et al., 1994), Rag2$^{-/-}$ (Hao and Rajewsky, 2001), Rorc$^{-/-}$ (Eberl et al., 2004) Rorc-EGFP (Lochner et al., 2008), and Tnfrs11a$^{-/-}$ (Li et al., 2000) mice have been described previously. Aire$^{-/-}$ and Adig mice were backcrossed onto a BALB/c background for ≥10 generations. Animal studies were approved by local authorities (Regierung von Oberbayern Az. 02–17-193 and Ethical Committee of the Czech Academy of Sciences).

Preparation of LN single-cell suspension

Unless stated otherwise, experiments were performed with pooled pLNs (axillary, brachial, inguinal, and cervical). LNs were pierced with a needle and enzymatically digested with 0.1 mg/ml Dispase (Gibco) in RPMI. After incubation at 37°C for 10 min, the supernatant was replenished, and cell suspensions were homogenized by gently pipetting up and down. To stop the digestion, the supernatant was adjusted to 3% FCS and 2 mM EDTA and gently spun down (4°C, 300 *g*, 5 min). The procedure was repeated until all clumping was removed. In the experiment shown in Fig. S3, LNs were digested in the presence of 0.5 U/ml Liberase (Roche). The cell suspensions were then resuspended in PBS containing 3% FCS and 2 mM EDTA and used for further analysis.

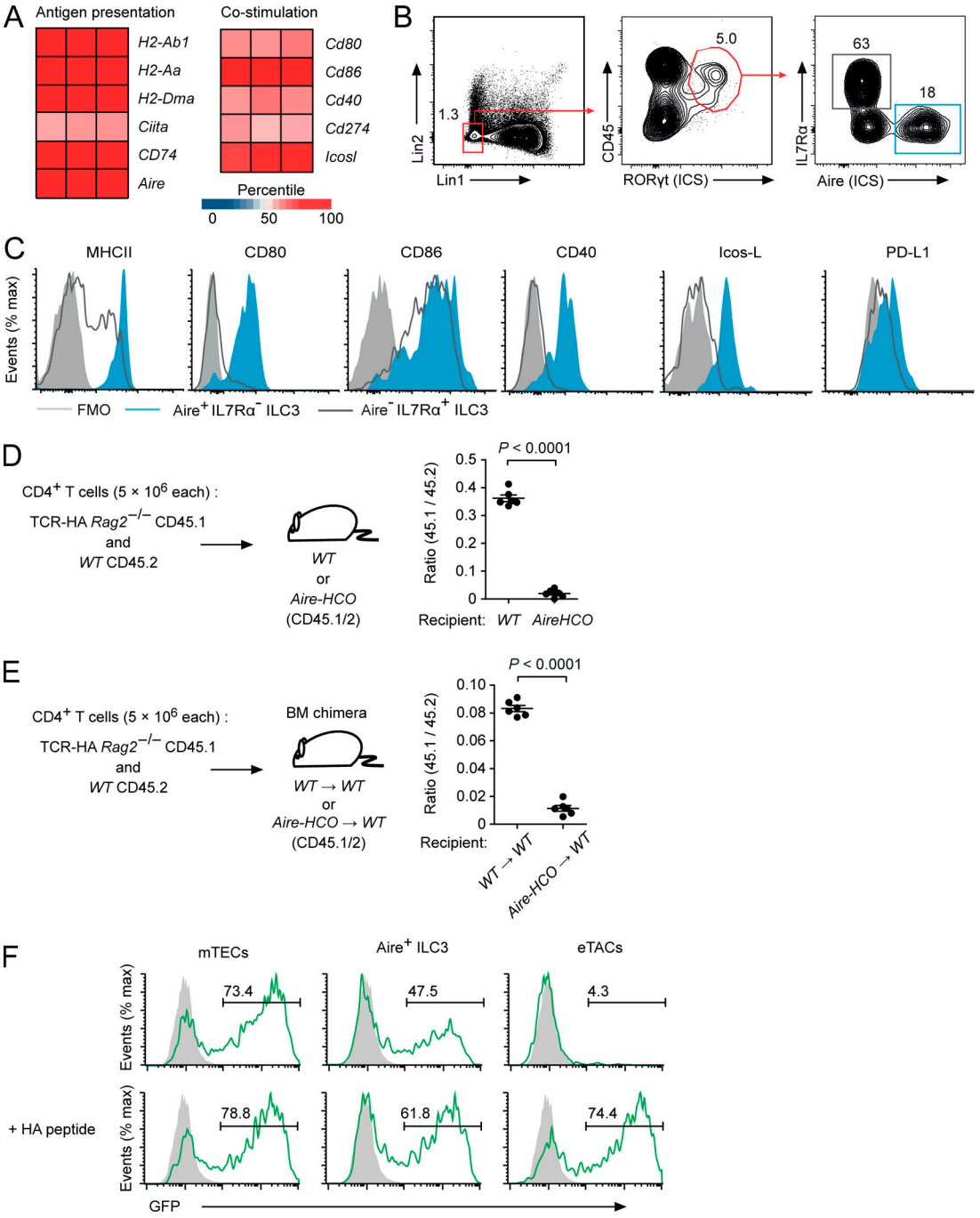

Figure 5. **Aire⁺ ILC3-like cells display potent APC features and directly present endogenous antigen on MHCII. (A)** RNA expression of genes involved in antigen presentation in Aire⁺ ILC3s. **(B)** Frequency of Aire⁺IL7Rα⁻ and Aire⁻IL7Rα⁺ cells among Lin⁻RORγt-ICS⁺CD45⁺ cells in pLNs (Lin1: CD3, CD19, B220, Gr-1; Lin 2: CD11c and CD11b). **(C)** Surface expression of MHCII and costimulatory molecules on Aire⁺IL7Rα⁻ (filled blue) or Aire⁻IL7Rα⁺ (open black) Lin⁻RORγt-ICS⁺CD45⁺ pLN cells (representative of $n \geq 3$). **(D)** Peripheral deletion of HA-specific CD4 T cells upon adoptive transfer into *Aire-HCO* mice ($n = 6$ each). **(E)** Peripheral deletion of HA-specific CD4 T cells upon adoptive transfer into [*Aire-HCO* → *WT*] BM chimeric mice ($n = 6$ each). **(F)** GFP expression in HA-specific CD4⁺ NFAT-GFP-reporter hybridoma cells after 16 h co-culture with mTECs, Aire⁺ ILC3-like cells (Aire-hCD2⁺MHCII⁺CD11c⁻EpCAM⁻), or eTACS (Aire-hCD2⁺MHCII⁺CD11c⁺EpCAM⁺) from Aire–HCO mice without (upper row) or with (lower row) exogenous HA-peptide. Filled gray histograms are from A5 cells that were cultured alone (representative of three experimental replicates). Data are mean ± SEM. Student's *t* test was used to calculate P values.

Flow cytometry

Single-cell suspensions of digested LNs were surface stained according to standard procedures. For intracellular Aire or RORγt staining, cells were fixed and permeabilized using reagents from the Foxp3 staining kit (eBioscience) and stained with anti-Aire mAb 5H12 (eBioscience) conjugated to Alexa Fluor 660, Alexa Fluor 488, or FITC- or PE-conjugated RORγt mAb B2D (eBioscience). Cells were analyzed or sorted using a BD FACSCANTOII or LSRII flow cytometer or BD FACSAriaFusion or BD Influx cell sorters.

Imaging flow cytometry

LN cells were prepared by enzymatic digestion. Thymic stroma cells were prepared by enzymatic digestion and density fractionation. Cells were stained for surface markers, fixed and permeabilized, and stained with Alexa Fluor 488–conjugated anti-Aire mAb 5H12 (eBioscience). DAPI was added immediately before analysis. Images were acquired using the ImageStream imaging flow cytometer (Amnis), and data were analyzed with the Ideas 6.0 software.

In vitro stimulation of ILC3s

LN cells from Aire-HCO mice were prepared by enzymatic digestion. B cells and T cells were depleted with biotin-conjugated anti-B220, anti-TCRβ, and anti-biotin MicroBeads (Miltenyi Biotech). Lineage-negative (CD3, CD11c, and CD19), hCD2-negative, IL7Rα$^+$MHCII$^+$-positive cells were sorted. Sorted cells (4×10^4) were cultured for 3 d together with 2×10^4 irradiated (3,000 rad) ST2 or ST2-RankL (Nutt et al., 1999) mouse BM stroma cells in flat-bottom 96-well plates. Where indicated, agonistic anti-CD40 mAb (10 µg/ml; FGK45; Bio X Cell) was added.

RNA-seq

Total mRNA was extracted from Lin$^-$CD45$^+$MHCII^{high}CD80$^+$ cells using the RNeasy Plus Microkit (Qiagen). The quality of the isolated RNA was controlled by Bioanalyzer 2100 electrophoresis (Agilent). RNA-seq libraries were prepared by the European Molecular Biology Laboratory Genomics core facility in Heidelberg, Germany using a NEXTflex rapid illumina RNA-Seq library prep kit (Bioo Scientific) after polyA enrichment with NEXTflex Poly(A) Beads (Bioo Scientific), starting with ∼1–5 pg of total RNA. Sequencing was performed on an Illumina NextSeq 500 sequencer (Illumina). Low quality reads and adaptor sequences were trimmed out using cutadapt. Reads mapping to ribosomal RNA were filtered out using SortMeRNA. Preprocessed mRNA reads were mapped to the mouse genome (BALB/cJ) from Ensembl version 86 (Mus_musculus_balbcj.BALB_cJ_v1.dna_sm.toplevel.fa) using GSNAP version 2017–02-25. Gene annotations were downloaded from Ensembl (Mus_musculus_balbcj.BALB_cJ_v1.86.gff3). DESeq2 version 1.14.1 was used for feature counting, data normalization, and comparison of the different groups. Differentially expressed genes were selected based on Storey's q-value < 0.05 and at least 1.5-fold change in transcription activity. For the construction of heat maps, fragments per kilobase of transcript per million mapped reads–normalized counts were used. The raw sequencing data were deposited at the ArrayExpress database under accession no. E-MTAB-7088.

Quantitative PCR

Total mRNA was extracted from cells using the RNeasy Plus Microkit (Qiagen). Reverse transcription was performed using random primers (Thermo Fisher Scientific) and RevertAid reverse transcription (Thermo Fisher Scientific). Gene expression was determined by quantitative PCR reaction using Sybr green and LC480-II cycler (Roche) and quantified using the relative quantification method (Pfaffl, 2001).

Antigen-presentation assay

10^4 HA-TCR hybridoma cells (A5 cells) were co-cultured with 2×10^3 APCs in 200 µl IMDM supplemented with 1% FCS. After 17 h, cells were harvested, and GFP expression of A5 cells was measured by flow cytometry.

BM and fetal liver chimeras

BM was depleted of B and T cells using biotinylated mAbs to B220 and TCRβ and streptavidin magnetic activated cell sorting beads (Miltenyi Biotech). Recipient mice were irradiated with 2×450 rad and reconstituted with 1×10^7 BM cells. For the generation of mixed chimeras, congenically marked BM or fetal liver cells from Rag2$^{-/-}$ (CD45.1$^{+/+}$), MHCII$^{-/-}$, RORc$^{-/-}$, CD40$^{-/-}$, or Tnfrsf11a$^{-/-}$ mice (CD45.2$^{+/+}$), and BM or fetal liver cells from WT mice of matching congenic genotype, were mixed at a ratio of 1:1 (5×10^6 each) and intravenously injected into lethally irradiated recipient mice (CD45.1$^{+/-}$CD45.2$^{+/-}$).

Adoptive T cell transfer

Single cell suspensions of LN cells from HA-TCR-RAG2$^{-/-}$ (CD45.1) and WT mice (CD45.2) were prepared. LN T cells from WT mice were enriched with biotin-conjugated anti-CD4 and streptavidin MicroBeads (Miltenyi Biotech) according to standard procedures. LN T cells were mixed (5×10^6) at a ratio of 1:1 and i.v. injected into recipient mice (CD45.1$^{+/-}$ CD45.2$^{+/-}$). After 14 d, the LNs were collected and single cell suspensions were analyzed by flow cytometry.

Statistical analysis

Unless indicated otherwise, statistical significance was assessed using the two-tailed Student's *t* test.

Online supplemental material

Fig. S1 shows the phenotype of Aire-expressing LN cells. Fig. S2 shows gating strategies. Fig. S3 shows that MHCII^{high}IL7Rα$^-$ ILC3-like cells express Aire$^-$ and costimulatory molecules. Table S1 shows Aire-induced genes in Aire$^+$ ILC3-like cells. Table S2 shows Aire-repressed genes in Aire$^+$ ILC3-like cells.

Acknowledgments

We thank C. Federle for expert technical assistance. We also thank L. Richter (FlowCyt Core Facility, BioMedical Center, Munich, Germany) and Z. Cimburek and M. Sima (Flow Cytometry Unit, Institute of Molecular Genetics, Prague, Czech Republic) for Flow Cytometry and Imaging Cytometry support, and M.S. Anderson (University of California, San Francisco, San Francisco, CA) for *Adig* mice.

This work was supported by the Deutsche Forschungsgemeinschaft (KL 1228/6-1 and SFB 1054, project parts A01 and IRTG, to L. Klein, T. Yamano, N. Ziętara, and M. Steinert) and the Grant Agency of Czech Republic (16-26143S to D. Filipp). T. Yamano was supported by the Leading Initiative for Excellent Young Researchers from the Japan Society for the Promotion of Science. J. Dobeš was supported by the Grant Agency of Charles University (900214) and a European Federation of Immunological Societies short-term fellowship. R. Sedláček was supported by grants funded by the Ministry of Education, Youth,

and Sports (LM2015040, CZ.1.05/2.1.00/19.0395, and LQ1604) and the European Regional Development Fund (OP RDE CZ.1.05/2.1.00/19.0395).

The authors declare no competing financial interests.

Author contributions: T. Yamano and J. Dobeš carried out the majority of experiments. M. Vobořil, M. Steinert, T. Brabec, N. Ziętara, and M. Dobešová contributed to individual experiments. C. Ohnmacht, M. Laan, P. Peterson, R. Sedláček, and R. Hanayama provided mice and material. V. Benes conducted the RNA-seq library preparation and sequencing. M. Kolář conducted the RNA-seq analysis. L. Klein and D. Filipp designed experiments and wrote the manuscript.

Submitted: 27 July 2018
Revised: 17 January 2019
Accepted: 27 February 2019

References

Adamson, K.A., S.H. Pearce, J.R. Lamb, J.R. Seckl, and S.E. Howie. 2004. A comparative study of mRNA and protein expression of the autoimmune regulator gene (Aire) in embryonic and adult murine tissues. *J. Pathol.* 202:180–187. https://doi.org/10.1002/path.1493

Akiyama, T., Y. Shimo, H. Yanai, J. Qin, D. Ohshima, Y. Maruyama, Y. Asaumi, J. Kitazawa, H. Takayanagi, J.M. Penninger, et al. 2008. The tumor necrosis factor family receptors RANK and CD40 cooperatively establish the thymic medullary microenvironment and self-tolerance. *Immunity.* 29:423–437. https://doi.org/10.1016/j.immuni.2008.06.015

Akiyama, T., M. Shinzawa, and N. Akiyama. 2012. TNF receptor family signaling in the development and functions of medullary thymic epithelial cells. *Front. Immunol.* 3:278. https://doi.org/10.3389/fimmu.2012.00278

Anderson, M.S., E.S. Venanzi, L. Klein, Z. Chen, S.P. Berzins, S.J. Turley, H. von Boehmer, R. Bronson, A. Dierich, C. Benoist, and D. Mathis. 2002. Projection of an immunological self shadow within the thymus by the aire protein. *Science.* 298:1395–1401. https://doi.org/10.1126/science.1075958

Anderson, M.S., E.S. Venanzi, Z. Chen, S.P. Berzins, C. Benoist, and D. Mathis. 2005. The cellular mechanism of Aire control of T cell tolerance. *Immunity.* 23:227–239. https://doi.org/10.1016/j.immuni.2005.07.005

Aschenbrenner, K., L.M. D'Cruz, E.H. Vollmann, M. Hinterberger, J. Emmerich, L.K. Swee, A. Rolink, and L. Klein. 2007. Selection of Foxp3+ regulatory T cells specific for self antigen expressed and presented by Aire+ medullary thymic epithelial cells. *Nat. Immunol.* 8:351–358. https://doi.org/10.1038/ni1444

Bando, J.K., S. Gilfillan, C. Song, K.G. McDonald, S.C. Huang, R.D. Newberry, Y. Kobayashi, D.S.J. Allan, J.R. Carlyle, M. Cella, and M. Colonna. 2018. The Tumor Necrosis Factor Superfamily Member RANKL Suppresses Effector Cytokine Production in Group 3 Innate Lymphoid Cells. *Immunity.* 48:1208–1219.e4. https://doi.org/10.1016/j.immuni.2018.04.012

Eberl, G., S. Marmon, M.J. Sunshine, P.D. Rennert, Y. Choi, and D.R. Littman. 2004. An essential function for the nuclear receptor RORgamma(t) in the generation of fetal lymphoid tissue inducer cells. *Nat. Immunol.* 5:64–73. https://doi.org/10.1038/ni1022

Fergusson, J.R., M.D. Morgan, M. Bruchard, L. Huitema, B.A. Heesters, V. van Unen, J.P. van Hamburg, N.N. van der Wel, D. Picavet, F. Koning, et al. 2019. Maturing Human CD127+ CCR7+ PDL1+ Dendritic Cells Express AIRE in the Absence of Tissue Restricted Antigens. *Front. Immunol.* 9:2902. https://doi.org/10.3389/fimmu.2018.02902

Fletcher, A.L., V. Lukacs-Kornek, E.D. Reynoso, S.E. Pinner, A. Bellemare-Pelletier, M.S. Curry, A.R. Collier, R.L. Boyd, and S.J. Turley. 2010. Lymph node fibroblastic reticular cells directly present peripheral tissue antigen under steady-state and inflammatory conditions. *J. Exp. Med.* 207:689–697. https://doi.org/10.1084/jem.20092642

Fujikado, N., A.O. Mann, K. Bansal, K.R. Romito, E.M.N. Ferre, S.D. Rosenzweig, M.S. Lionakis, C. Benoist, and D. Mathis. 2016. Aire Inhibits the Generation of a Perinatal Population of Interleukin-17A-Producing γδ T Cells to Promote Immunologic Tolerance. *Immunity.* 45:999–1012. https://doi.org/10.1016/j.immuni.2016.10.023

Gardner, J.M., J.J. Devoss, R.S. Friedman, D.J. Wong, Y.X. Tan, X. Zhou, K.P. Johannes, M.A. Su, H.Y. Chang, M.F. Krummel, and M.S. Anderson. 2008. Deletional tolerance mediated by extrathymic Aire-expressing cells. *Science.* 321:843–847. https://doi.org/10.1126/science.1159407

Gardner, J.M., A.L. Fletcher, M.S. Anderson, and S.J. Turley. 2009. AIRE in the thymus and beyond. *Curr. Opin. Immunol.* 21:582–589. https://doi.org/10.1016/j.coi.2009.08.007

Gardner, J.M., T.C. Metzger, E.J. McMahon, B.B. Au-Yeung, A.K. Krawisz, W. Lu, J.D. Price, K.P. Johannes, A.T. Satpathy, K.M. Murphy, et al. 2013. Extrathymic Aire-expressing cells are a distinct bone marrow-derived population that induce functional inactivation of CD4+ T cells. *Immunity.* 39:560–572. https://doi.org/10.1016/j.immuni.2013.08.005

Gray, D., J. Abramson, C. Benoist, and D. Mathis. 2007. Proliferative arrest and rapid turnover of thymic epithelial cells expressing Aire. *J. Exp. Med.* 204:2521–2528. https://doi.org/10.1084/jem.20070795

Gury-BenAri, M., C.A. Thaiss, N. Serafini, D.R. Winter, A. Giladi, D. Lara-Astiaso, M. Levy, T.M. Salame, A. Weiner, E. David, et al. 2016. The Spectrum and Regulatory Landscape of Intestinal Innate Lymphoid Cells Are Shaped by the Microbiome. *Cell.* 166:1231–1246.e13. https://doi.org/10.1016/j.cell.2016.07.043

Haljasorg, U., R. Bichele, M. Saare, M. Guha, J. Maslovskaja, K. Kõnd, A. Remm, M. Pihlap, L. Tomson, K. Kisand, et al. 2015. A highly conserved NF-κB-responsive enhancer is critical for thymic expression of Aire in mice. *Eur. J. Immunol.* 45:3246–3256. https://doi.org/10.1002/eji.201545928

Halonen, M., M. Pelto-Huikko, P. Eskelin, L. Peltonen, I. Ulmanen, and M. Kolmer. 2001. Subcellular location and expression pattern of autoimmune regulator (Aire), the mouse orthologue for human gene defective in autoimmune polyendocrinopathy candidiasis ectodermal dystrophy (APECED). *J. Histochem. Cytochem.* 49:197–208. https://doi.org/10.1177/002215540104900207

Hao, Z., and K. Rajewsky. 2001. Homeostasis of peripheral B cells in the absence of B cell influx from the bone marrow. *J. Exp. Med.* 194:1151–1164. https://doi.org/10.1084/jem.194.8.1151

Heino, M., P. Peterson, N. Sillanpää, S. Guérin, L. Wu, G. Anderson, H.S. Scott, S.E. Antonarakis, J. Kudoh, N. Shimizu, et al. 2000. RNA and protein expression of the murine autoimmune regulator gene (Aire) in normal, RelB-deficient and in NOD mouse. *Eur. J. Immunol.* 30:1884–1893. https://doi.org/10.1002/1521-4141(200007)30:7<1884::AID-IMMU1884>3.0.CO;2-P

Hepworth, M.R., L.A. Monticelli, T.C. Fung, C.G. Ziegler, S. Grunberg, R. Sinha, A.R. Mantegazza, H.L. Ma, A. Crawford, J.M. Angelosanto, et al. 2013. Innate lymphoid cells regulate CD4+ T-cell responses to intestinal commensal bacteria. *Nature.* 498:113–117. https://doi.org/10.1038/nature12240

Hepworth, M.R., T.C. Fung, S.H. Masur, J.R. Kelsen, F.M. McConnell, J. Dubrot, D.R. Withers, S. Hugues, M.A. Farrar, W. Reith, et al. 2015. Immune tolerance. Group 3 innate lymphoid cells mediate intestinal selection of commensal bacteria-specific CD4+ T cells. *Science.* 348:1031–1035. https://doi.org/10.1126/science.aaa4812

Hikosaka, Y., T. Nitta, I. Ohigashi, K. Yano, N. Ishimaru, Y. Hayashi, M. Matsumoto, K. Matsuo, J.M. Penninger, H. Takayanagi, et al. 2008. The cytokine RANKL produced by positively selected thymocytes fosters medullary thymic epithelial cells that express autoimmune regulator. *Immunity.* 29:438–450. https://doi.org/10.1016/j.immuni.2008.06.018

Hinterberger, M., M. Aichinger, O. Prazeres da Costa, D. Voehringer, R. Hoffmann, and L. Klein. 2010. Autonomous role of medullary thymic epithelial cells in central CD4(+) T cell tolerance. *Nat. Immunol.* 11:512–519. https://doi.org/10.1038/ni.1874

Hubert, F.X., S.A. Kinkel, K.E. Webster, P. Cannon, P.E. Crewther, A.I. Proeitto, L. Wu, W.R. Heath, and H.S. Scott. 2008. A specific anti-Aire antibody reveals aire expression is restricted to medullary thymic epithelial cells and not expressed in periphery. *J. Immunol.* 180:3824–3832. https://doi.org/10.4049/jimmunol.180.6.3824

Hubert, F.X., S.A. Kinkel, G.M. Davey, B. Phipson, S.N. Mueller, A. Liston, A.I. Proietto, P.Z. Cannon, S. Forehan, G.K. Smyth, et al. 2011. Aire regulates the transfer of antigen from mTECs to dendritic cells for induction of thymic tolerance. *Blood.* 118:2462–2472. https://doi.org/10.1182/blood-2010-06-286393

Husebye, E.S., M.S. Anderson, and O. Kämpe. 2018. Autoimmune Polyendocrine Syndromes. *N. Engl. J. Med.* 378:2543–2544. https://doi.org/10.1056/NEJMra1713301

Irla, M., S. Hugues, J. Gill, T. Nitta, Y. Hikosaka, I.R. Williams, F.X. Hubert, H.S. Scott, Y. Takahama, G.A. Holländer, and W. Reith. 2008. Autoantigen-specific interactions with CD4+ thymocytes control mature medullary thymic epithelial cell cellularity. *Immunity.* 29:451–463. https://doi.org/10.1016/j.immuni.2008.08.007

Jones, R., E.J. Cosway, C. Willis, A.J. White, W.E. Jenkinson, H.J. Fehling, G. Anderson, and D.R. Withers. 2018. Dynamic changes in intrathymic ILC populations during murine neonatal development. *Eur. J. Immunol.* 48: 1481–1491. https://doi.org/10.1002/eji.201847511

Kawabe, T., T. Naka, K. Yoshida, T. Tanaka, H. Fujiwara, S. Suematsu, N. Yoshida, T. Kishimoto, and H. Kikutani. 1994. The immune responses in CD40-deficient mice: impaired immunoglobulin class switching and germinal center formation. *Immunity.* 1:167–178. https://doi.org/10.1016/1074-7613(94)90095-7

Kirberg, J., A. Baron, S. Jakob, A. Rolink, K. Karjalainen, and H. von Boehmer. 1994. Thymic selection of CD8+ single positive cells with a class II major histocompatibility complex-restricted receptor. *J. Exp. Med.* 180:25–34. https://doi.org/10.1084/jem.180.1.25

Klein, L., B. Kyewski, P.M. Allen, and K.A. Hogquist. 2014. Positive and negative selection of the T cell repertoire: what thymocytes see (and don't see). *Nat. Rev. Immunol.* 14:377–391. https://doi.org/10.1038/nri3667

Kuroda, N., T. Mitani, N. Takeda, N. Ishimaru, R. Arakaki, Y. Hayashi, Y. Bando, K. Izumi, T. Takahashi, T. Nomura, et al. 2005. Development of autoimmunity against transcriptionally unrepressed target antigen in the thymus of Aire-deficient mice. *J. Immunol.* 174:1862–1870. https://doi.org/10.4049/jimmunol.174.4.1862

Kyewski, B., and L. Klein. 2006. A central role for central tolerance. *Annu. Rev. Immunol.* 24:571–606. https://doi.org/10.1146/annurev.immunol.23.021704.115601

Laan, M., K. Kisand, V. Kont, K. Möll, L. Tserel, H.S. Scott, and P. Peterson. 2009. Autoimmune regulator deficiency results in decreased expression of CCR4 and CCR7 ligands and in delayed migration of CD4+ thymocytes. *J. Immunol.* 183:7682–7691. https://doi.org/10.4049/jimmunol.0804133

LaFlam, T.N., G. Seumois, C.N. Miller, W. Lwin, K.J. Fasano, M. Waterfield, I. Proekt, P. Vijayanand, and M.S. Anderson. 2015. Identification of a novel cis-regulatory element essential for immune tolerance. *J. Exp. Med.* 212:1993–2002. https://doi.org/10.1084/jem.20151069

Lei, Y., A.M. Ripen, N. Ishimaru, I. Ohigashi, T. Nagasawa, L.T. Jeker, M.R. Bösl, G.A. Holländer, Y. Hayashi, R.W. Malefyt, et al. 2011. Aire-dependent production of XCL1 mediates medullary accumulation of thymic dendritic cells and contributes to regulatory T cell development. *J. Exp. Med.* 208:383–394. https://doi.org/10.1084/jem.20102327

Li, J., I. Sarosi, X.Q. Yan, S. Morony, C. Capparelli, H.L. Tan, S. McCabe, R. Elliott, S. Scully, G. Van, et al. 2000. RANK is the intrinsic hematopoietic cell surface receptor that controls osteoclastogenesis and regulation of bone mass and calcium metabolism. *Proc. Natl. Acad. Sci. USA.* 97:1566–1571. https://doi.org/10.1073/pnas.97.4.1566

Lochner, M., L. Peduto, M. Cherrier, S. Sawa, F. Langa, R. Varona, D. Riethmacher, M. Si-Tahar, J.P. Di Santo, and G. Eberl. 2008. In vivo equilibrium of proinflammatory IL-17+ and regulatory IL-10+ Foxp3+ RORgamma t+ T cells. *J. Exp. Med.* 205:1381–1393. https://doi.org/10.1084/jem.20080034

Luci, C., A. Reynders, I.I. Ivanov, C. Cognet, L. Chiche, L. Chasson, J. Hardwigsen, E. Anguiano, J. Banchereau, D. Chaussabel, et al. 2009. Influence of the transcription factor RORgammat on the development of NKp46+ cell populations in gut and skin. *Nat. Immunol.* 10:75–82. https://doi.org/10.1038/ni.1681

Mathis, D., and C. Benoist. 2007. A decade of AIRE. *Nat. Rev. Immunol.* 7: 645–650. https://doi.org/10.1038/nri2136

Montaldo, E., K. Juelke, and C. Romagnani. 2015. Group 3 innate lymphoid cells (ILC3s): Origin, differentiation, and plasticity in humans and mice. *Eur. J. Immunol.* 45:2171–2182. https://doi.org/10.1002/eji.201545598

Nishikawa, Y., F. Hirota, M. Yano, H. Kitajima, J. Miyazaki, H. Kawamoto, Y. Mouri, and M. Matsumoto. 2010. Biphasic Aire expression in early embryos and in medullary thymic epithelial cells before end-stage terminal differentiation. *J. Exp. Med.* 207:963–971. https://doi.org/10.1084/jem.20092144

Nutt, S.L., B. Heavey, A.G. Rolink, and M. Busslinger. 1999. Commitment to the B-lymphoid lineage depends on the transcription factor Pax5. *Nature.* 401:556–562. https://doi.org/10.1038/44076

Peterson, P., T. Org, and A. Rebane. 2008. Transcriptional regulation by AIRE: molecular mechanisms of central tolerance. *Nat. Rev. Immunol.* 8: 948–957. https://doi.org/10.1038/nri2450

Pfaffl, M.W. 2001. A new mathematical model for relative quantification in real-time RT-PCR. *Nucleic Acids Res.* 29:e45. https://doi.org/10.1093/nar/29.9.e45

Poliani, P.L., K. Kisand, V. Marrella, M. Ravanini, L.D. Notarangelo, A. Villa, P. Peterson, and F. Facchetti. 2010. Human peripheral lymphoid tissues contain autoimmune regulator-expressing dendritic cells. *Am. J. Pathol.* 176:1104–1112. https://doi.org/10.2353/ajpath.2010.090956

Ramsey, C., O. Winqvist, L. Puhakka, M. Halonen, A. Moro, O. Kämpe, P. Eskelin, M. Pelto-Huikko, and L. Peltonen. 2002. Aire deficient mice develop multiple features of APECED phenotype and show altered immune response. *Hum. Mol. Genet.* 11:397–409. https://doi.org/10.1093/hmg/11.4.397

Roberts, N.A., A.J. White, W.E. Jenkinson, G. Turchinovich, K. Nakamura, D. R. Withers, F.M. McConnell, G.E. Desanti, C. Benezech, S.M. Parnell, et al. 2012. Rank signaling links the development of invariant γδ T cell progenitors and Aire(+) medullary epithelium. *Immunity.* 36:427–437. https://doi.org/10.1016/j.immuni.2012.01.016

Robinette, M.L., A. Fuchs, V.S. Cortez, J.S. Lee, Y. Wang, S.K. Durum, S. Gilfillan, and M. Colonna. Immunological Genome Consortium. 2015. Transcriptional programs define molecular characteristics of innate lymphoid cell classes and subsets. *Nat. Immunol.* 16:306–317. https://doi.org/10.1038/ni.3094

Rossi, S.W., M.Y. Kim, A. Leibbrandt, S.M. Parnell, W.E. Jenkinson, S.H. Glanville, F.M. McConnell, H.S. Scott, J.M. Penninger, E.J. Jenkinson, et al. 2007. RANK signals from CD4(+)3(-) inducer cells regulate development of Aire-expressing epithelial cells in the thymic medulla. *J. Exp. Med.* 204:1267–1272. https://doi.org/10.1084/jem.20062497

Sansom, S.N., N. Shikama-Dorn, S. Zhanybekova, G. Nusspaumer, I.C. Macaulay, M.E. Deadman, A. Heger, C.P. Ponting, and G.A. Holländer. 2014. Population and single-cell genomics reveal the Aire dependency, relief from Polycomb silencing, and distribution of self-antigen expression in thymic epithelia. *Genome Res.* 24:1918–1931. https://doi.org/10.1101/gr.171645.113

Satoh-Takayama, N., L. Dumoutier, S. Lesjean-Pottier, V.S. Ribeiro, O. Mandelboim, J.C. Renauld, C.A. Vosshenrich, and J.P. Di Santo. 2009. The natural cytotoxicity receptor NKp46 is dispensable for IL-22-mediated innate intestinal immune defense against Citrobacter rodentium. *J. Immunol.* 183:6579–6587. https://doi.org/10.4049/jimmunol.0901935

Schaller, C.E., C.L. Wang, G. Beck-Engeser, L. Goss, H.S. Scott, M.S. Anderson, and M. Wabl. 2008. Expression of Aire and the early wave of apoptosis in spermatogenesis. *J. Immunol.* 180:1338–1343. https://doi.org/10.4049/jimmunol.180.3.1338

Seehus, C.R., P. Aliahmad, B. de la Torre, I.D. Iliev, L. Spurka, V.A. Funari, and J. Kaye. 2015. The development of innate lymphoid cells requires TOX-dependent generation of a common innate lymphoid cell progenitor. *Nat. Immunol.* 16:599–608. https://doi.org/10.1038/ni.3168

Spits, H., D. Artis, M. Colonna, A. Diefenbach, J.P. Di Santo, G. Eberl, S. Koyasu, R.M. Locksley, A.N. McKenzie, R.E. Mebius, et al. 2013. Innate lymphoid cells--a proposal for uniform nomenclature. *Nat. Rev. Immunol.* 13:145–149. https://doi.org/10.1038/nri3365

von Burg, N., S. Chappaz, A. Baerenwaldt, E. Horvath, S. Bose Dasgupta, D. Ashok, J. Pieters, F. Tacchini-Cottier, A. Rolink, H. Acha-Orbea, and D. Finke. 2014. Activated group 3 innate lymphoid cells promote T-cell-mediated immune responses. *Proc. Natl. Acad. Sci. USA.* 111:12835–12840. https://doi.org/10.1073/pnas.1406908111

Wang, X., M. Laan, R. Bichele, K. Kisand, H.S. Scott, and P. Peterson. 2012. Post-Aire maturation of thymic medullary epithelial cells involves selective expression of keratinocyte-specific autoantigens. *Front. Immunol.* 3:19. https://doi.org/10.3389/fimmu.2012.00019

Yamano, T., J. Nedjic, M. Hinterberger, M. Steinert, S. Koser, S. Pinto, N. Gerdes, E. Lutgens, N. Ishimaru, M. Busslinger, et al. 2015. Thymic B Cells Are Licensed to Present Self Antigens for Central T Cell Tolerance Induction. *Immunity.* 42:1048–1061. https://doi.org/10.1016/j.immuni.2015.05.013

Yano, M., N. Kuroda, H. Han, M. Meguro-Horike, Y. Nishikawa, H. Kiyonari, K. Maemura, Y. Yanagawa, K. Obata, S. Takahashi, et al. 2008. Aire controls the differentiation program of thymic epithelial cells in the medulla for the establishment of self-tolerance. *J. Exp. Med.* 205: 2827–2838. https://doi.org/10.1084/jem.20080046